

Understanding and Predicting El Niño and the Southern Oscillation

Michael J. McPhaden

NOAA/Pacific Marine Environmental Laboratory, Seattle, WA, USA

This chapter reviews basic concepts about the El Niño/Southern Oscillation (ENSO) cycle and its global climatic impacts. It also highlights progress in understanding, observing, and predicting ENSO timescale variations, focusing on the 2015–16 El Niño as a case study. This El Niño was one of the strongest on record; its evolution and many of its far-field impacts were remarkably well predicted at lead times of 6–9 months. Despite progress to date, however, there are many outstanding issues that need to be addressed to improve our understanding and ability to predict ENSO.

Introduction

ENSO is the most prominent year-to-year climate fluctuation affecting the globe. It originates in the tropical Pacific through coupled ocean-atmosphere interactions mediated by wind and sea surface temperature (SST) feedbacks (Fig. 23.1). We refer to the warm phase of ENSO as El Niño and the cold phase as La Niña; individual events recur roughly every 2–7 years. Its influence extends worldwide through atmospheric teleconnections that shift the probabilities for drought, flood, heat waves, and other extreme weather events (Fig. 23.2).

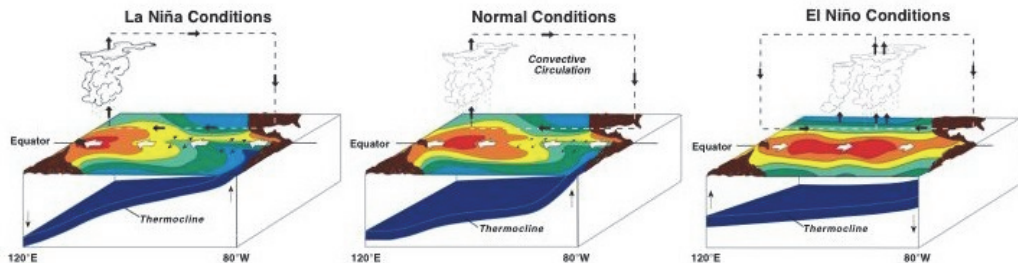


Figure 23.1. A schematic of La Niña, normal and El Niño conditions in the tropical Pacific.

ENSO is the largest source of predictability in the climate system on seasonal timescales, other than the normal march of the seasons. Over the past 30 years, there have been major advances in our understanding of ENSO variations and their impacts, in the development of ocean observing systems to support ENSO prediction, and in the development of seasonal forecast models capable of skillful forecasts with lead times of 6–9 months. Satellites, moored buoys (the so-called TAO-

TRITON array in the Pacific), Argo floats, and other measurement systems (Fig. 23.3) provide critical data for developing improved forecast models and for initializing and validating those models.

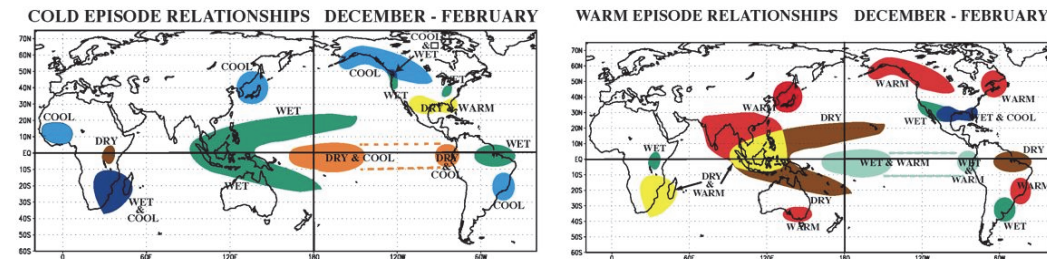


Figure 23.2. Summary of La Niña (left) and El Niño (right) climate impacts in terms of temperature and precipitation for December–February, which is the season of ENSO event peak development. Figure courtesy of NOAA Climate Prediction Center.

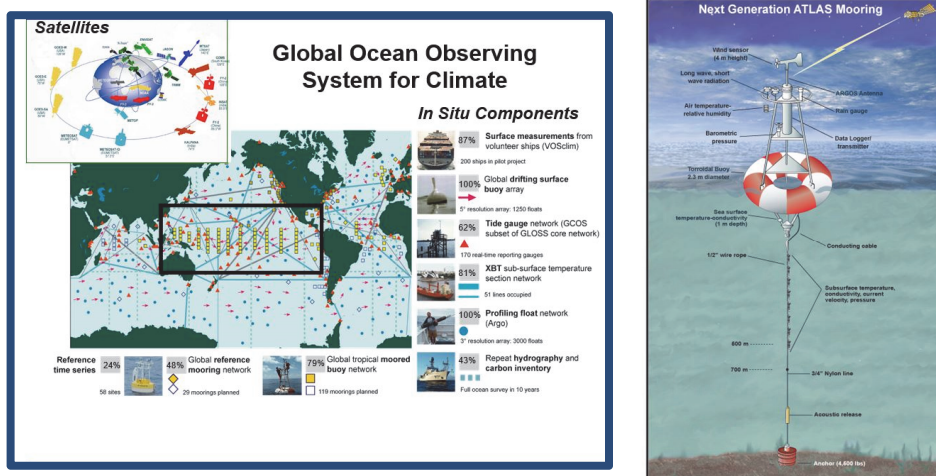


Figure 23.3. Schematic of the Global Ocean Observing System for Climate (left) with the tropical Pacific outlined. The TAO/TRITON array (yellow squares in the tropical Pacific) was implemented specifically for ENSO research and forecasting. ATLAS moorings (right) or their equivalent, which provide oceanic and atmospheric data in real-time via satellite relay, make up the majority of TAO/TRITON moorings.

The 2015–16 El Niño

The 2015–16 El Niño was of comparable magnitude to the other two major El Niños in the historical record (1982–83 and 1997–98) and one of the strongest on record (McPhaden, 2015; L’Heureux et al., 2017). Thus, it provides a timely case study for highlighting advances in understanding, observing, and predicting El Niño and its impacts. Typical of most El Niños, the event developed early in the calendar year, reached its peak development in the boreal winter, and terminated in the following spring (Fig. 23.4). With the large-scale collapse of the trade winds in 2015, the western Pacific warm pool (surface water $>28\text{--}29^{\circ}\text{C}$) migrated eastward along the equator, the thermocline flattened out, and the normally cold upwelled water that forms the equatorial “cold tongue” in the eastern Pacific was only weakly evident at the height of the event in December 2015 (Fig. 23.5).

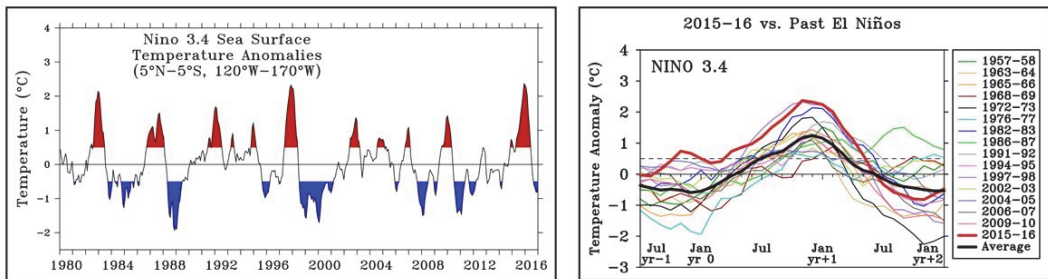


Figure 23.4. Monthly mean values of the Nino3.4 SST index since 1980 (left) for El Niño events (red peaks above 0.5°C threshold) and La Niña events (blue troughs below 0.5°C threshold). Comparative amplitudes of El Niños in the Nino3.4 region since the late 1950s (right) based on 2.5-year segments of the Nino3.4 record centered on the season of peak development in boreal winter. The thick black line is the average of 14 El Niños during this time, excluding 2015–16, which is shown as a thick red line. The dashed horizontal line is the 0.5°C threshold for El Niño. Nino3.4 SST is one of the most commonly used ENSO indices because of strong ocean-atmosphere coupling on seasonal timescales in this region (shown in Fig. 23.5) and because of the robust relationship between Nino3.4 SST variations and global climate impacts. The Nino3.4 time series were not detrended in this figure since trends are weak in this particular region. Base period for computing anomalies is 1981–2010.

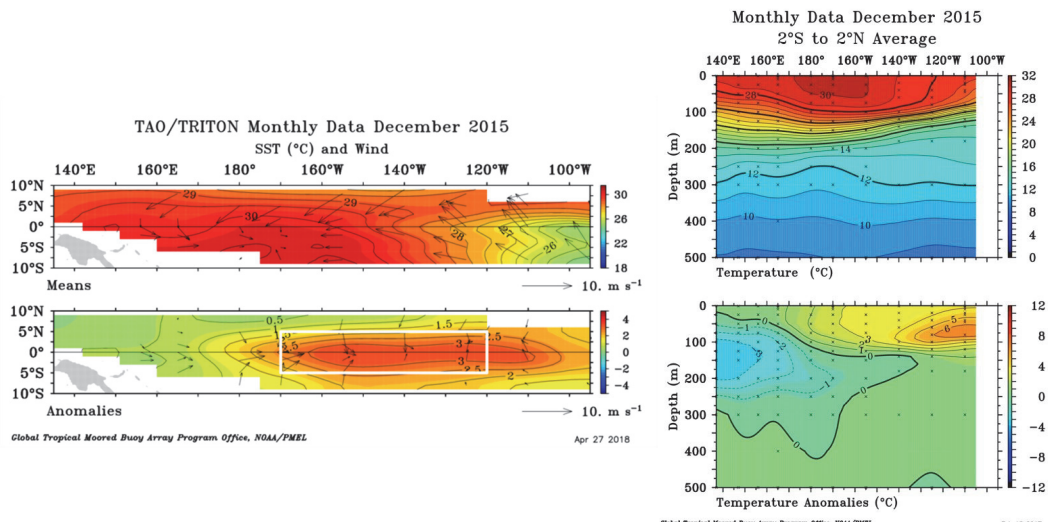


Figure 23.5. Monthly means and anomalies of surface winds and SST (left) and subsurface temperature along the equator (right) from the TAO/TRITON array for December 2015 at the height of the 2015–16 El Niño. The Nino3.4 region is outlined in the anomaly plot of the left panel. More information about gridding procedures and base periods for computing anomalies can be found at www.pmel.noaa.gov/gtmba.

A comparison of SST anomalies for December 1997, 2009, and 2015 (Fig. 23.6) illustrates the concept of ENSO diversity (Capotondi et al., 2015). All El Niños are characterized by warmer than normal SSTs and weakened trade winds along the equator but the location of maximum SST anomalies can vary significantly from event to event. For example, compared to the previous major El Niño of 1997–98 (which has been referred to as an “eastern Pacific” or EP El Niño), SST anomalies were shifted westward along the equator in 2015–16 and reached historical highs west of the Nino3.4 region (Xue and Kumar, 2017). However, compared to the 1997–98 El Niño, SST anomalies were weaker east of about 140°W in December 2015. The 2009–10 El Niño, a “central

Pacific” or CP El Niño, was different from either of these other two El Niños, with the largest warm anomalies confined to the central Pacific and very little warming in the eastern Pacific cold tongue. Compared to 1997–98 and 2009–10, the 2015–16 event appears to be a hybrid between these two types of El Niño (L’Heureux et al., 2017; Paek et al., 2017). The details of these SST patterns are important because they can affect atmospheric teleconnections and climate impacts associated with different El Niño events (Capotondi et al., 2015).

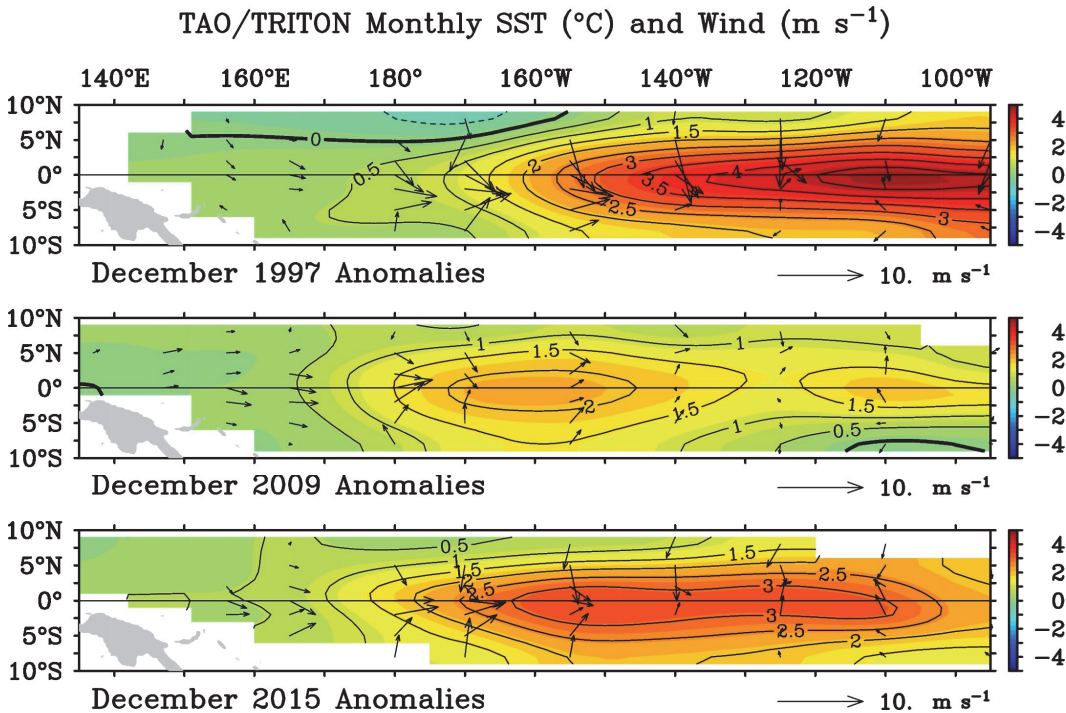


Figure 23.6. Comparison of surface wind and SST anomalies for December 1997, 2009, and 2015. The 1997–98 El Niño was an eastern Pacific (EP) event while 2009–10 was a central Pacific (CP) event. The 2014–15 El Niño appears to be a hybrid of these two types of El Niño.

The 2015–16 El Niño also illustrates the interplay between large-scale deterministic seasonal timescale dynamics associated with theories such as the recharge oscillator (Jin, 1997) and delayed oscillator (e.g., Battisti, 1988; Schopf and Suarez, 1988) and higher frequency stochastic processes. Collapse of the trade winds during El Niño in particular is very episodic, punctuated by a series of westerly wind bursts (Fig. 23.7a) that lead to warming along the equator in the central and eastern Pacific. Warming in the central Pacific in 2015 (Fig. 23.7b) was caused by very strong eastward wind-driven flows that advected the western Pacific warm pool eastward. Episodic westerly wind forcing also generated downwelling equatorial Kelvin waves that crossed the basin in about 45 days (Fig. 23.7c), leaving in their wake a thermocline depressed by up to 40 m so as to reduce the efficiency of equatorial upwelling to cool the surface. The net effect of these processes was to shift the locus of warm surface water eastward and with it deep atmospheric convection. Positive feedbacks between the ocean and the atmosphere reinforced the surface warming and the weakening trade winds, which allowed the El Niño to grow to a large amplitude. Delayed negative feedbacks

in the form of an upwelling Kelvin wave along the equator in early 2016 began to lift the thermocline, eventually initiating surface cooling on the onset of a weak La Niña. This Kelvin wave may have emanated from the western boundary, consistent with delayed oscillator theory, or have been forced by easterly wind anomalies in the far western Pacific, or some combination of both these effects.

It is also noteworthy that the westerly wind bursts in 2015 appear to be mostly confined to the region west of the 29 °C isotherm and disappear as the western Pacific cools in 2016. Thus, the stochastic forcing of ENSO is not completely random but depends on the state of ENSO itself. This is referred to as state-dependent noise forcing and it is an important element of ENSO dynamics (Eisenmann et al., 2015; Levine and McPhaden, 2016).

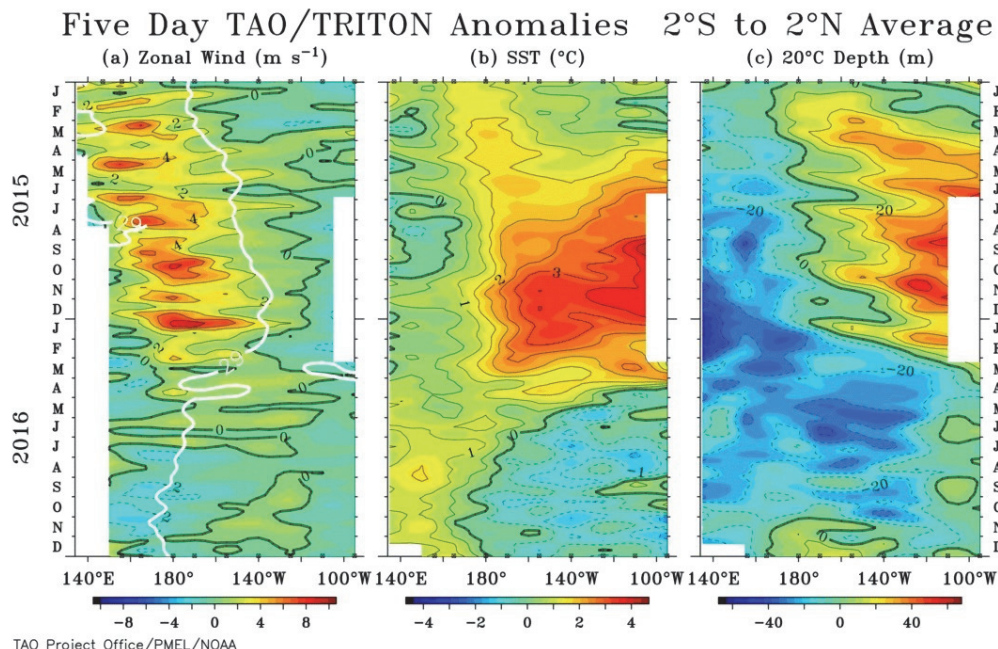


Figure 23.7. Five-day analyses of (a) zonal wind, (b) SST, and (c) 20 °C depth anomalies averaged 2°N–2°S based on TAO/TRITON moored time series data for 2015–16. The depth of the 20 °C isotherm is a measure of the depth of the thermocline. The white line in the left panel shows the longitudinal position of the 29 °C SST isotherm, which is an indication of the eastern edge of the western Pacific warm pool. Dots on the upper and lower axes show longitudes where data are available. More information about gridding procedures and base periods for computing anomalies can be found at www.pmel.noaa.gov/gtmfa.

It has long been known that a build-up of excess heat content along the equator preconditions the tropical Pacific to the development of El Niño and that heat content is a useful predictor of ENSO development (Jin, 1997; Meinen and McPhaden, 2000). This concept is illustrated by comparing Niño3.4 SST with upper ocean heat content as measured by the depth averaged temperature anomaly in the upper 300 m integrated from the coast of western South America to the coast of New Guinea between 5°N and 5°S. Heat content leads Niño3.4 SST by typically 6–9 months except for during the first decade of the 21st century (McPhaden, 2012). Moreover, the largest build-up of heat content since 1980, other than that observed in 1997, occurred in 2015 prior

to the full development of the 2015–16 El Niño. With such a strong build-up of heat content, one might have anticipated the development of a strong El Niño.

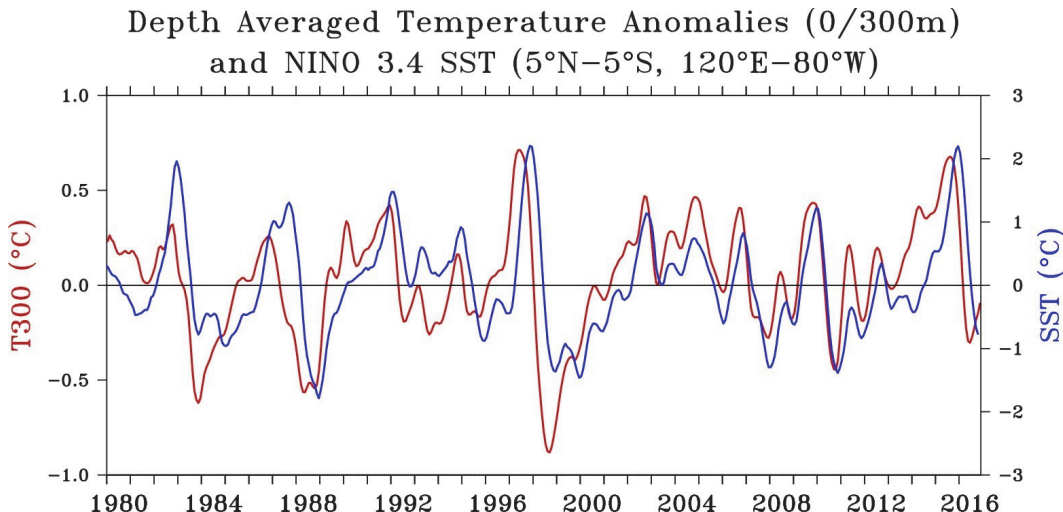


Figure 23.8. Time series of Nino3.4 SST and anomalous ocean heat content along the equator (T300) between 1980 and 2016. Monthly means have been smoothed with a five-month running mean.

Forecast models used to predict ENSO range include purely statistical models, hybrid statistical-dynamical models, and coupled global ocean-atmosphere general circulation models. Seasonal forecasts of Nino3.4 SSTs from these models, beginning in mid-2015, were more accurate than for any event since 2002 when systematic tracking of skill scores for multi-model ensembles began (L’Heureux et al., 2017). As an example, forecasts initialized in July 2015 verified extremely well as an ensemble against the observations over the next year (Fig. 23.9). Global precipitation forecasts also verified well in many regions of the globe at the peak of the event (December 2015–February 2016), with the notable exception of the west coast of the United States (Fig. 23.10). Overall, El Niño forcing from the tropical Pacific could account for about 25% of the variance in seasonal mean precipitation anomalies during the peak of the event (L’Heureux et al., 2017). On the other hand, the highly anticipated rains that El Niño was supposed to bring to California after several years of severe drought failed to materialize. Kumar and Chen (2017) have suggested this failed forecast may simply have been due to chance, given the high degree of random variability in seasonal rainfall totals along the west coast of the U.S. even in the face of strong El Niño forcing from the tropical Pacific.

Summary

Advances in understanding, observing system development, and forecast model development have made skillful ENSO forecasts routinely possible 2–3 seasons in advance. Successful prediction of the 2015–16 El Niño and its impacts demonstrate these advances. Even so, many challenges remain. For example, while seasonal forecasts for 2015–16 were very successful, this is not always the case. Predictive skill was low in the first decade of the 21st century (Barnston et al., 2012) and notably

low in 2014, when a highly anticipated strong El Niño failed to develop (McPhaden, 2015). Understanding what factors limit ENSO predictability is thus a major outstanding issue.

A related question involves the processes that give rise to ENSO diversity. Various hypotheses have been proposed, such as variations in stochastic forcing (Levine et al., 2016), decadal changes in the background state of the tropical Pacific (Choi et al., 2012), and forcing from regions outside the tropical Pacific (Paek et al., 2017). How these and other factors may combine to influence the evolution of individual events is a subject of great interest given that diversity in ENSO characteristics can result in a diversity of climatic impacts.

Mid-Aug 2015 Plume of Model ENSO Predictions

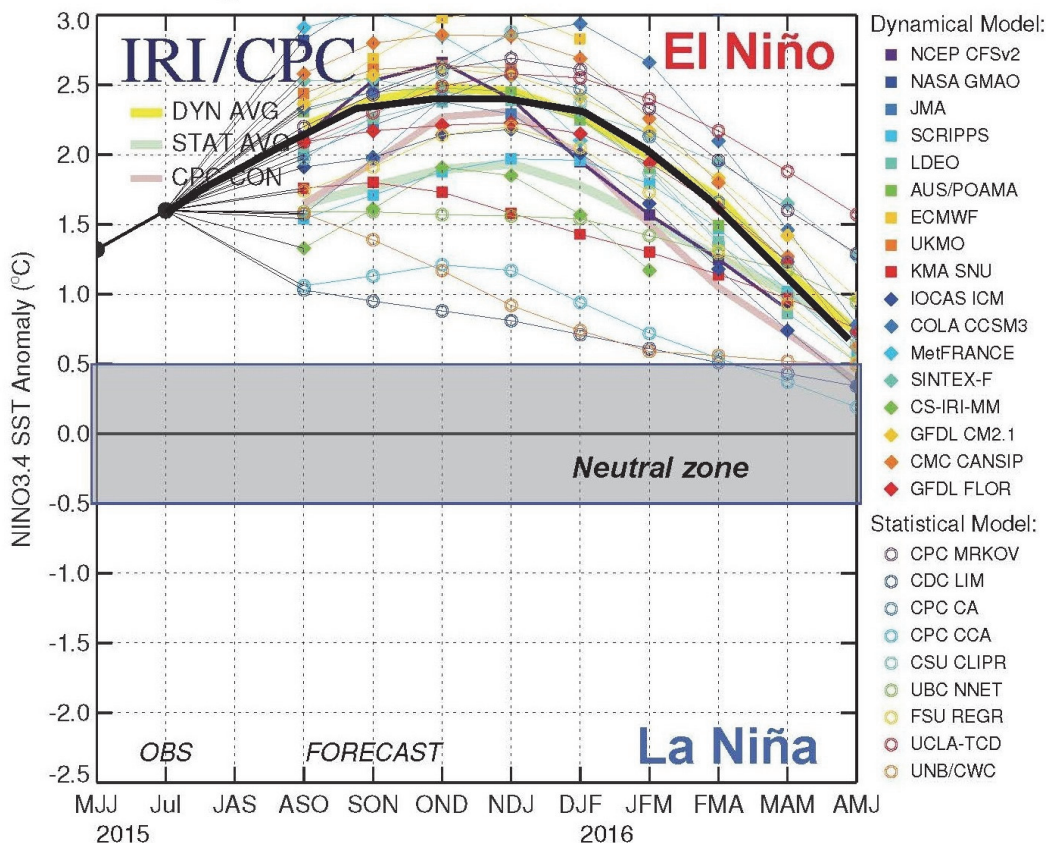


Figure 23.9. Forecasts of seasonal mean Nino3.4 SST anomalies using different forecast models for July 2015 initial conditions. Thick solid black line is the verification. Adapted from the International Research Institute for Climate and Society.

There is also the question of whether global warming has already affected the ENSO cycle and how it will affect it in the future. This is an area of lively debate but much uncertainty. Analysis of historical data, paleoclimate records, and numerical model simulations often lead to conflicting results. Perhaps the most robust conclusion so far is that in a warmer world the frequency of extreme El Niños like those observed in 1982–83, 1997–98, and 2015–16 will increase in the future (Cai et

al., 2014). But much more work needs to be done on this topic, which is a rich and fertile ground for further research.

Finally, the TAO/TRITON array, which was designed in the 1980s and implemented over the 10-year period 1985–94, has served as the cornerstone of the tropical Pacific Ocean observing system for the past 30 years (McPhaden et al., 2010). Data from the moored buoy array are distributed via the Global Telecommunications System to operational centers around the globe for routine ocean, weather, and climate forecasting. They also serve as a primary dataset for many oceanic and atmospheric databases and for virtually all oceanic and atmospheric reanalysis products. Since the 1980s, there have been advances in our understanding of the processes involved in ENSO dynamics and new technologies such as Argo profiling floats have become available. As a result of these developments, an international committee is currently reviewing the design of the tropical Pacific Ocean Observing System, with recommendations for how to optimize it for the 21st century still pending (Cravatte et al., 2016).

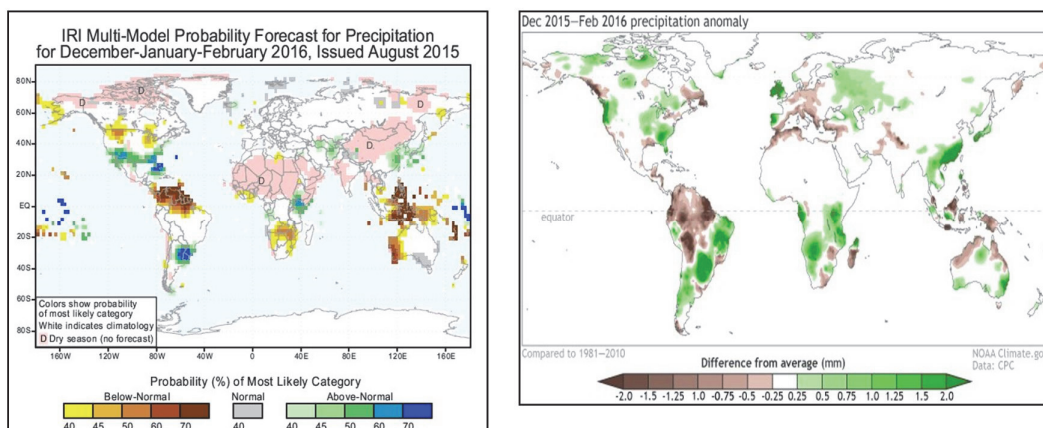


Figure 23.10. Precipitation forecasts for December 2015–February 2016 based on August 2015 initial conditions (left). Actual rainfall anomalies for December 2015–February 2016 (right). Forecasts and observed anomalies are courtesy of the International Research Institute for Climate and Society (<https://iri.columbia.edu>).

References

- Barnston, A. G., M. K. Tippett, M. L. L’Heureux, S. Li, and D. G. DeWitt, 2012: Skill of real-time seasonal ENSO model predictions during 2002–11: Is our capability increasing? *Bull. Amer. Meteor. Soc.*, 93, 631–651.
- Battisti, D. S., 1988: Dynamics and thermodynamics of a warming event in a coupled atmosphere-ocean model, *J. Atmos. Sci.*, 45, 2889–2919.
- Cai, W., S. Borlace, M. Lengaigne, P. van Renssch, M. Collins, G. Vecchi, A. Timmermann, M. J. McPhaden, L. Wu, M. England, E. Guilyardi, and F.-F. Jin, 2014: Increasing frequency of extreme El Niño events due to greenhouse warming. *Nature Climate Change*, 4, 111–116.
- Capotondi et al., 2015: Understanding ENSO diversity. *Bull. Am. Meteorol. Soc.*, 96, 921–938.
- Choi, J., S.-I. An, and S. W. Yeh, 2012: Decadal amplitude modulation of two types of ENSO and its relationship with the mean state. *Clim. Dyn.*, doi:10.1007/s00382-011-1186-y.
- Cravatte, S., W. S. Kessler, N. Smith, S. E. Wijffels, and Contributing Authors, 2016: First Report of TPOS 2020. GOOS-215, 200 pp. (<http://tpos2020.org/first-report/>)
- Eisenman, I., L. Yu, and E. Tziperman, 2005: Westerly wind bursts: ENSO’s tail rather than the dog? *J. Clim.*, 18, 5224–5238.

- Jin, F.F., 1997: An equatorial recharge paradigm for ENSO. Part I: Conceptual model. *J. Atmos. Sci.*, 54, 811–829.
- Kumar, A. and M. Chen, 2017: What is the variability in US west coast winter precipitation during strong El Niño events? *Clim. Dyn.*, 49, 2789–2802.
- Levine, A. F. Z. and M. J. McPhaden, 2016: How the July 2014 easterly wind burst gave the 2015–2016 El Niño a head start. *Geophys. Res. Lett.*, 43, 6503–6510.
- Levine, A.F.Z., F.F. Jin, M.J. McPhaden, 2016: Extreme noise-extreme El Niño: How state-dependent noise forcing creates El Niño-La Niña asymmetry. *J. Climate*, 29, 5483–5499.
- L’Heureux, M. et al., 2017: Observing and predicting the 2015/16 El Niño. *Bull. Am. Meteorol. Soc.*, 98, 1363–1382.
- McPhaden, M. J., A. J. Busalacchi, and D. L. T. Anderson, 2010a: A TOGA retrospective. *Oceanography*, 23, 86–103.
- McPhaden, M. J., 2012: A 21st Century Shift in the Relationship between ENSO SST and Warm Water Volume Anomalies. *Geophys. Res. Lett.*, 39, L09706, doi:10.1029/2012GL051826.
- McPhaden M J. 2015: Playing hide and seek with El Niño. *Nat Clim Change*, 5, 791–795
- Meinen, C.S. and M.J. McPhaden, 2000: Observations of warm water volume changes in the equatorial Pacific and their relationship to El Niño and La Niña. *J. Climate*, 13, 3551–3559.
- Paek, H., J.-Y. Yu, and C. Qian, 2017: Why were the 2015/16 and 1997/98 Extreme El Niños different? *Geophys. Res. Lett.*, 44, 1848–1856.
- Suarez, M. J., and P. S. Schopf, 1988: A delayed action oscillator for ENSO, *J. Atmos. Sci.*, 45, 3283–3287.
- Xue, Y. and A. Kumar, 2017: Evolution of the 2015/16 El Niño and historical perspective since 1979. *Science China*, 60, 1572–1588.